Alkylammonium-Functionalized Hollow Mesoporous Silica Nanocarrier for Cancer Therapy

Sung Soo Park and Chang-Sik Ha *

Posted Date: 24 August 2023

doi: 10.20944/preprints202308.1656.v1

Keywords: Hollow mesoporous silica; Alkylammonium; Fludarabine; Drug delivery; Cancer therapy

Article

Alkylammonium-Functionalized Hollow Mesoporous Silica Nanocarrier for Cancer Therapy

Sung Soo Park [1] and Chang-Sik Ha [2,*]

[1] Division of Advanced Materials Engineering, Dong-Eui University, Busan 47340, Republic of Korea; pss@deu.ac.kr (S.S.P.)

[2] Department of Polymer Science and Engineering, School of Chemical Engineering, Pusan National University, Busan 46241, Republic of Korea; csha@pusan.ac.kr (C.-S.H.)

* Correspondence: csha@pusan.ac.kr (C.-S.H.).

Abstract: In this work, alkylammonium-functionalized hollow mesoporous silica as nonocarrier of drugs was synthesized to realize enhanced cancer therapy by pH stimuli for sustained drug release. First, functionalized hollow mesoporous silica nanoparticles (Hollow MSNs) were synthesized using dodecyl dimethyl(3-sulfopropyl)ammonium hydroxide (DDAPS), sodium dodecyl sulfate (SDS), and triethanolamine as structure-directing agents, and tetraethyl orthosilicate (TEOS) and N-trimethoxysilypropyl-N,N,N-trimethylammonium chloride (TMAPS) as silica sources under basic condition via the sol-gel process. The structure and morphology of the alkylammonium-functionalized hollow mesoporous silica nanoparticles (Hollow MSN-N^+CH_3) were characterized by X-ray diffraction (XRD), scanning electron microscopy (SEM), transmission electron microscopy (TEM), N_2 adsorption-desorption analysis, and Fourier-transform infrared (FT-IR) spectroscopy. The functionalized hollow MSNs had a particle size of about 450 nm and a shell thickness of about 60 nm with uniform size. The nanoparticle had a surface area of 408 m^2g^{-1}, pore volume of 0.8 cm^3g^{-1} and a uniform pore diameter of 45.9 Å. In the cancer cell viability test with MCF-7 cell, fludarabine-incorporated and alkylammonium-functionalized hollow mesoporous silica nanoparticles (Flu/Hollow MSN-N^+CH_3) showed excellent cancer cell death comparable with pure fludarabine drug with the controlled drug release by pH stimuli. It is considered that our current materials have the potential applicability as pH-responsive nanocarriers in the field of cancer therapy.

Keywords: hollow mesoporous silica; alkylammonium; fludarabine; drug delivery; cancer therapy

1. Introduction

Drug delivery technologies have made a significant contribution to the development of many pharmaceutical products that improve patients' health by improving drug delivery to the target site and delivering the right amount of drug [1]. Currently, targeted therapy, which uses nanoparticles as a delivery system in cancer treatment to ensure site-specific delivery and release of drugs, is receiving a lot of attention and is being actively studied by many researchers [2-4].

Meanwhile, controlled drug release along with efficient drug delivery to the target is also very important for maximizing treatment. Injecting high doses of drugs into the human body can cause damage to healthy organs or tissues in humans by causing undesirable interactions between the drugs and normal cells [5,6]. Therefore, many researchers are making great efforts to overcome these disadvantages by using a controlled drug delivery system [7,8]. Stimuli-responsive polymers [9,10], hydrogels, and many types of inorganic nanoparticles [6,11,12] are being actively studied using temperature, light irradiation, pH, redox, etc. as external stimuli for drug release control without any device.

In recent years, among various drug delivery systems, mesoporous silica nanoparticles (MSNs) are receiving great attention in the field of controlled drug delivery because of easy synthesis and surface functionalization, tunable pore size, large surface area, and biocompatibility [13-15]. The MSNs have silica walls and uniform nanopores, so they can protect drugs or other compounds and

 doi:10.20944/preprints202308.1656.v1

prevent leakage with excellent biocompatibility and high loading capacity [6,16]. Also, since MSNs can be easily functionalized on both the inner and outer surfaces, premature release of drugs or cargo from the pores can be prevented [6,17]. The MSNs were functionalized with various organic moieties such as aliphatic and aromatic groups including N, O, S atoms, and their derivatives to use as drug carriers with controlled release properties and toxicity to cancer cells [18-25]. The functionalized MSNs exhibited the controlled release behavior of drugs in nanopores by various stimuli such as pH, light, temperature, enzyme, redox, etc. [18-25].

Meanwhile, hollow mesoporous silica (HMS) nanoparticles have large pores in the core and nanopores in the shell. Therefore, they can be expected to have dual-drug delivery, high amount of drug loading, and different behavior of drug release due to the dual size of the pore. Many researchers have reported studies on controlled drug release and tests of cancer cell death using drug-incorporated HMS. Ma et al. [26] reported a study on the integrated hollow mesoporous silica nanoparticles for target Drug/siRNA Co-delivery. Liu et al. [27] reported on the single peptide ligand-functionalized uniform hollow mesoporous silica nanoparticles achieving dual-targeting drug delivery to tumor cells and angiogenic blood vessel cells. Chakravarty et al. [28] reported on hollow mesoporous silica nanoparticles for tumor vasculature targeting and positron emission tomography(PET) image-guided drug delivery. She et al. [29] reported on the functionalization of hollow mesoporous silica nanoparticles for improved 5-fluorouracil (5-FU) loading. Yang et al. [30] on the hollow silica nanocontainers as drug delivery vehicles. Xu et al. [31] reported on the facile way of fabricating PEGylated hollow mesoporous silica nanoparticles and their drug delivery application. Zhu et al. [32] reported on hollow mesoporous silica nanoparticles with tunable structures for controlled drug delivery. Liu et al. [33] reported on the redox-responsive hollow mesoporous silica nanoparticles that were constructed via host–guest interactions for controllable drug release. Nia et al. [34] reported on the biotemplated hollow mesoporous silica particles as efficient carriers for drug delivery. Recently, Li et al. [35] reported on the modified hollow mesoporous silica nanoparticles as immune adjuvant-nanocarriers for photodynamically enhanced cancer immunotherapy.

Cancer remains a challenge and leading cause of death for humans. Many studies using MSN as a drug carrier report results of controlled release of cancer drugs and toxicity studies on cancer cells [4,23,36-40]. In those studies, doxorubicin (Dox), 5-FU, paclitaxel (PTX), camptothecin (CPT), and epirubicin were mainly used as model drugs. Fludarabine phosphate is a synthetic purine nucleoside that inhibits DNA polymerase and is used for the treatment of chronic lymphocytic leukemia. On the other hand, to the best of our knowledge, few studies have been conducted on the controlled drug delivery systems with the functionalized mesoporous silica using fludarabine phosphate as a model drug.

In this context, alkylammonium-functionalized hollow mesoporous silica as nanocarrier of drugs was synthesized, to realize enhanced cancer therapy by pH stimuli for sustained drug release in this work. Fludarabine phosphate was used as a model drug for cytotoxicity testing on MCF-7 cells.

2. Experimental Section

2.1. Materials

The following reagents were used for this work. ; Dodecyl dimethyl(3-sulfopropyl)ammonium hydroxide (DDAPS, TCI, ≥98.0%), sodium dodecyl sulfate (SDS, Sigma-Aldrich, ≥99.0%) tetraethyl orthosilicate (TEOS, Sigma-Aldrich, 98%), N-trimethoxysilypropyl-N,N,N-trimethylammonium chloride (TMAPS, Gelest, 50% in methanol), triethanolamine (Sigma-Aldrich, 98%), ammonia aqueous solution (NH_4OH, Sigma-Aldrich, 25%), ethanol (anhydrous) (Junsei Chemical, 99%), hydrochloric acid (Matsunoen Chemicals Ltd., 35% in H_2O), and fludarabine (Sigma-Aldrich). All the reagents were used without further purification.

2.2. Synthesis of alkylammonium-functionalized hollow mesoporous silica

Preprints (www.preprints.org) | NOT PEER-REVIEWED | Posted: 24 August 2023 doi:10.20944/preprints202308.1656.v1

40 ml of an aqueous surfactant mixture was prepared with DDAPS/SDS=1:1 (mol ratio) (10 mM) in water. 1. 80 g of triethanolamine (12 mmol) and 1 ml of ammonia aqueous solution (2.5% NH_3 in H_2O) were added to the surfactant mixture solution. After stirring at room temperature for 1 h to obtain a homogeneous mixture, 630 µl of TEOS (2.8 mmol) and 224 µl of TMAPS (0.4 mmol) were added and heated at 45 °C for 30 min with stirring. The total mixture was heated at 80 °C for another 24 h under static condition. The obtained product was isolated, washed with water and ethanol several times by filtration, and dried in an oven at 80 °C for 24 h. The resulting product was designated as 'Hollow MSN-N^+CH_3 composite'. After this procedure, solvent extraction was conducted to remove the surfactant in the mesopores. Hollow MSN-N^+CH_3 composite was stirred in 150 ml of EtOH containing 3 ml of 35 wt% HCl aqueous solution at 60 °C for 12 h, and filtered and washed with EtOH. This process was repeated two times. The product was dried at 80 °C for 24 h. The sample was designated as 'Hollow MSN-N^+CH_3. The synthesis process was briefly shown in Scheme 1.

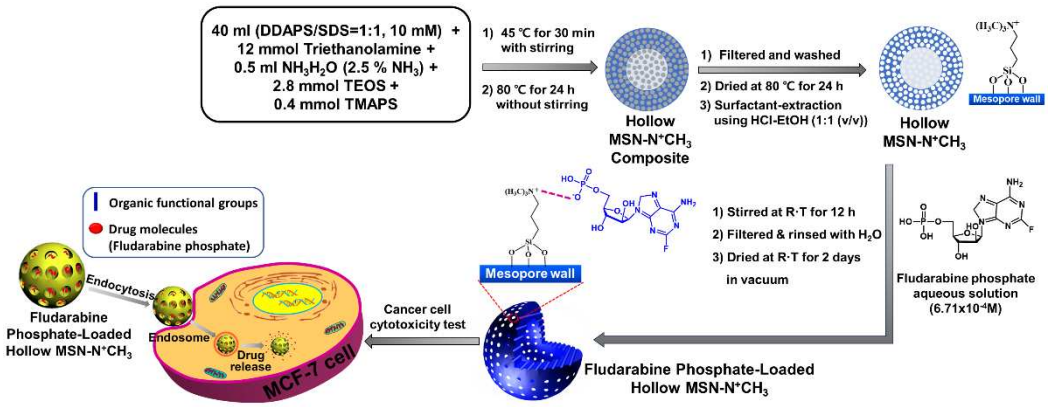

Scheme 1. An illustration for the preparation of Hollow MSN-N^+CH_3 and the cancer cell cytotoxicity test.

2.3. Synthesis of alkylammonium-functionalized and fludarabine-loaded hollow mesoporous silica

0.6 g of Hollow MSN-N^+CH_3 was suspended in 30 ml of 6.7 x 10^{-4} M-fludarabine (Flu) solution in H_2O and stirred at room temperature for 12 h. The solid sample was filtered and rinsed several times with H_2O and then dried at room temperature for 2 days in a vacuum oven (1 torr). The resulting product was designed as 'Flu/Hollow MSN-N^+CH_3'.

2.4. Drug releasing test

20 mg of Flu/Hollow MSN-N^+CH_3 was added to 5 ml of aqueous solution and the dispersion was filled into a dialysis bag (cutoff molecular weight (Mw) = 1.2 kDa). The bag with dispersion was immersed in 20 ml of aqueous solution of different pH (4.8, 7.4, 9.0) at 37 °C in a shaking incubator. At the specific time intervals, 2 ml of external medium was taken and replaced with the same volume of new aqueous solution immediately. The amount of released fludarabine (Flu) ($\%R_t$) was calculated by measuring intensity by a UV-vis spectrophotometer at 263 nm.

$$\%R_t = \frac{C_t \cdot V_1 + V_2 \cdot (C_{t-1} + C_{t-2} + \cdots + C_0)}{W_0 \cdot L} \times 100\% \quad (1)$$

The above equation was applied to calculate the drug release degree of samples. C_t is the drug concentration at time interval t; C_{t-1} + C_{t-2} are drug concentrations prior to time interval t (C_0 = 0); V_1 is the total volume of the release bath (25 ml), and V_2 is the volume extracted for UV-vis analysis (2 ml). W_0 is the initial weight of the Flu/Hollow MSN-N^+CH_3 and L is the drug loading capacity of the Flu/Hollow MSN-N^+CH_3 [41]. Also, calibration curves of fludarabine in aqueous solution at different pH (pH 4.8, 7.4, 9.0) were used to translate UV-vis intensity to the concentration of fludarabine (Flu) in the medium.

 doi:10.20944/preprints202308.1656.v1

2.5. Cell culture

Human breast adenocarcinoma (MCF-7) cell lines were maintained in Dulbecco's Modified Eagle's Medium (DMEM, Welgene, Korea) supplemented with 10% foetal bovine serum (FBS, Welgene, Korea) and 1% penicillinestreptomycin (Welgene, Korea) at 37 oC with 5% CO_2 in a 95% humidified atmosphere. Dulbecco's phosphate buffered saline (DPBS) was purchased from Welgene (Korea). For the cell viability tests, 3-(4,5-dimethylthiazol-2-yl)-2,5-diphenyltetrazolium bromide (MTT) was purchased from Sigma-Aldrich (St. Louis, MO, USA).

2.6. Measurements and characterization

X-ray powder diffraction (XRD, Rigaku Miniflex) was performed using Cu-Kα radiation (λ = 1.5418 Å) at 30 kV and 15 mA. The characteristic surface functional groups were analyzed by Fourier transform infrared spectroscopy (FTIR, JASCO (FTIR-4100)) at a scanning range of 400–4000 cm^{-1} in KBr. Transmission electron microscopy (TEM, TALOS F200X) was performed at an accelerating voltage of 200 kV. High resolution low voltage scanning electron microscopy (HRLV-SEM, JSM-7900F) was conducted at an operating voltage of 2.0 kV. The adsorption/desorption isotherms of nitrogen at 77 K were measured using a Nova 4000e surface area and pore size analyzer. Before starting the measurements, each sample was outgassed for 12 h under vacuum at 343K. The pore surface area was calculated by Brunauer-Emmet-Teller (BET) method and the pore size distribution curve was obtained from an analysis of the adsorption branch using the Barrette-Joynere-Halenda (BJH) method. Ultraviolet–visible (UV-vis) spectrophotometry (Hitachi U-2010) was used to measure the drug release rate.

3. Results and discussion

3.1. Synthesis of Hollow MSN-N^+CH_3 and Flu/Hollow MSN-N^+CH_3

Scheme 1 presents a schematic illustration of the synthesis of Hollow MSN-N^+CH_3 and Flu/Hollow MSN-N^+CH_3. First, The alkylammonium-functionalized hollow mesoporous silica was synthesized using dodecyl dimethyl(3-sulfopropyl)ammonium hydroxide (DDAPS), sodium dodecyl sulfate (SDS), and triethanolamine as structure-directing agents, and tetraethyl orthosilicate (TEOS) and N-trimethoxysilypropyl-N,N,N-trimethylammonium chloride (TMAPS) as silica sources under basic condition via the self-assembly and sol-gel reaction process by one-pot synthesis mehod. Drug molecules (Flu) were introduced on the surface of the pores by the electrostatic interaction between alkylammonium groups and drug molecules.

3.2. Characterization of Hollow MSN, Hollow MSN-N^+CH_3 and Flu/Hollow MSN-N^+CH_3

3.2.1. Scanning electron microscopy (SEM) and Transmission electron microscopy (TEM)

Figure 1 shows SEM (a, b) and TEM images (c) of Hollow MSN-N^+CH_3. The alkylammonium-functionalized hollow mesoporous silica (Hollow MSN-N^+CH_3) has a particle size of about 450 nm and a shell thickness of about 60 nm with uniform size as shown in TEM image (Figure 1c). The surfaces of the particles show rather rough surfaces with smaller particles. The TEM image showed the mesopores in the shell have an ordered 2D hexagonal mesostructure with parallel strips and uniform pore size [42-44], even after the surface of the mesopores was functionalized with alkylammonium groups. (Figure 1d)

Preprints (www.preprints.org) | NOT PEER-REVIEWED | Posted: 24 August 2023 doi:10.20944/preprints202308.1656.v1

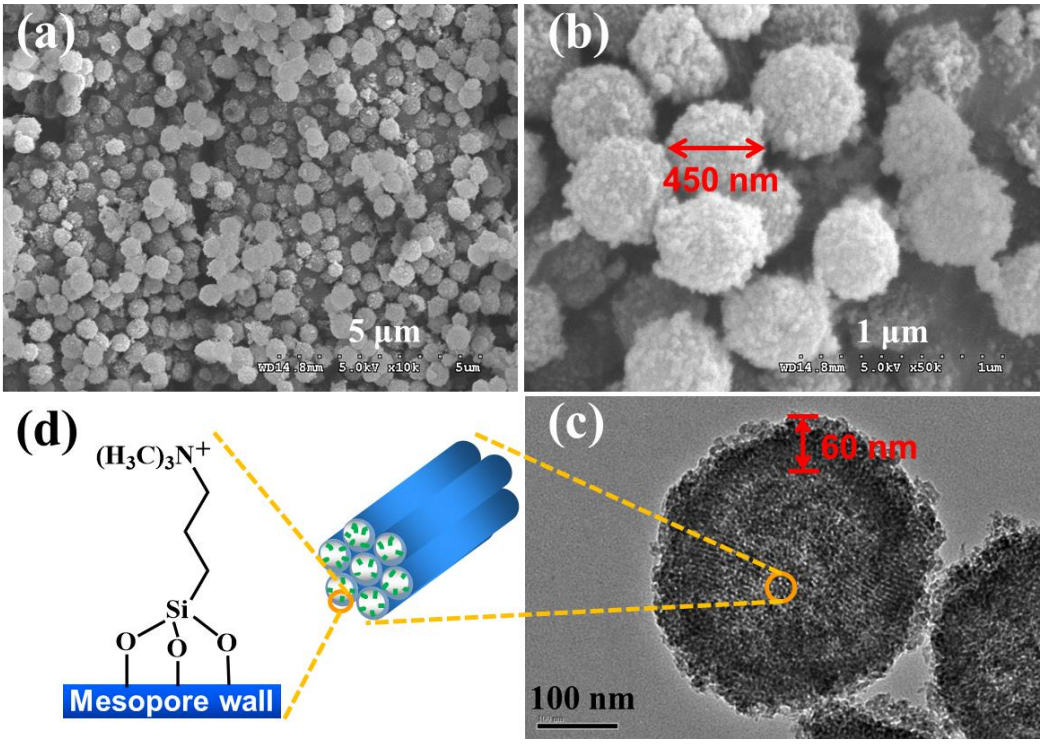

Figure 1. SEM (a, b) and TEM images (c) of Hollow MSN-N+CH3. (d) A schematic diagram of the alkylammonium-functionalized mesopore wall.

3.2.2. XRD patterns

Figure 2 shows XRD patterns of (a) Hollow MSN and (b) Hollow MSN-N^+CH_3. The alkylammonium-functionalized hollow mesoporous silica (Hollow MSN-N^+CH_3) shows one peak assigned by (100) reflection at $2\theta=1.44^o$ (Figure 2b). The (110), (200), and (210) reflections in the range of $2\theta=2.5\sim6^o$ seen on the 2D-hexagonal mesostructure are not clear due to the broad XRD pattern. The result indicates that the mesopores have an ordered structure in a small range [42-44]. However, it can be confirmed from the TEM image shown in Figure 1c that Hollow MSN-N^+CH_3 has uniformly sized mesopores despite less ordering. Here, to compare the usefulness of the alkylammonium groups in Hollow MSN-N^+CH_3, hollow mesoporous silica nanoparticles (Hollow MSN) without organic functional groups were prepared by calcination of Hollow MSN-N^+CH_3 at 550 °C for 4 h in air. Hollow MSN showed lower intensity and broader peaks compared to Hollow MSN-N^+CH_3 (Figure 2a). The result may be due to the disappearance of organic groups present in the pore walls and the collapse of the mesostructure due to shrinkage of the pore walls by treatment at high temperatures of 550 °C [45]. The 2θ values of Hollow MSN increased to 1.61^o. The result occurs by the shrinkage of the mesopore walls at high temperature [45].

Preprints (www.preprints.org) | NOT PEER-REVIEWED | Posted: 24 August 2023 doi:10.20944/preprints202308.1656.v1

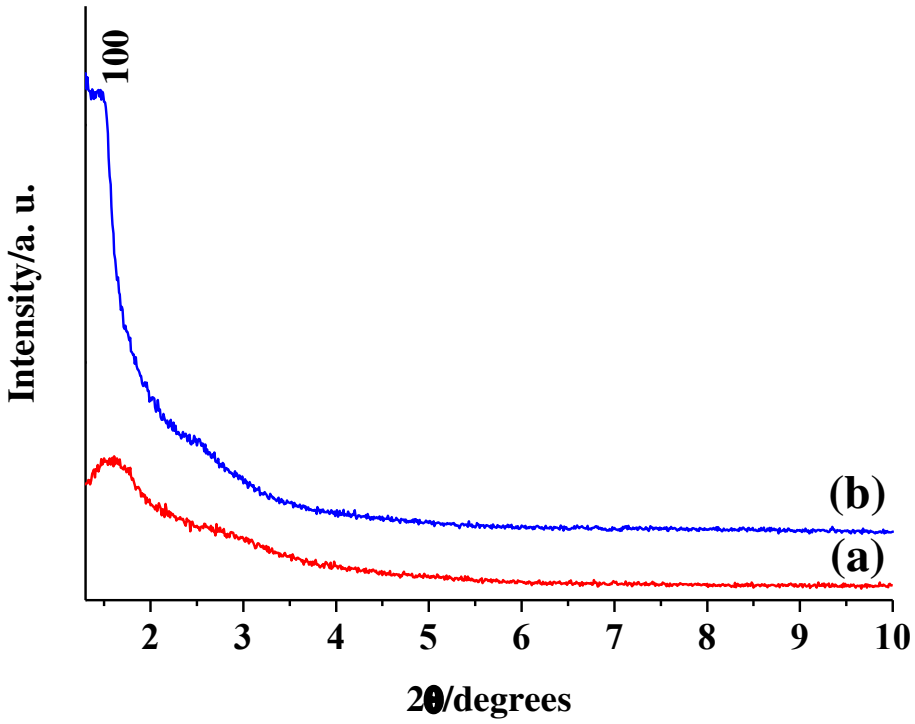

Figure 2. XRD patterns of (a) Hollow MSN and (b) Hollow MSN-N^+CH_3.

3.2.3. N_2 adsorption-desorption isotherms and pore size distributions

Figure 3 shows N_2 adsorption-desorption isotherms of (a) Hollow MSN and (b) Hollow MSN-N^+CH_3. Inset shows pore size distributions of (a) Hollow MSN and (b) Hollow MSN-N^+CH_3. Hollow MSN-N^+CH_3 have BET surface area of 405 m^2g^{-1} and pore volume of 0.80 cm^3g^{-1}. Pore diameter of Hollow MSN-N^+CH_3 was 45.9 Å. The result agrees well with the TEM image in Figure 1c. Also, the pore size distribution gradually increased to the right of the plot. The result is attributed to large pores in core of hollow nanoparticles and voids formed by aggregation of nanoparticles [18,46]. The pore diameter of Hollow MSN treated at high temperature was 39.4 Å, which is smaller than that of Hollow MSN-N^+CH_3. It is due to the shrinkage of the mesopores [45]. Also, as in the case of Hollow MSN-N^+CH_3, a broad pore size distribution was shown around 300 Å. BET surface area and pore volume of Hollow MSN were 358 m^2g^{-1} and 0.90 cm^3g^{-1}, respectively.

3.2.4. FT-IR spectra

Figure 4 shows FT-IR spectra of (a) Fludarabine phosphate, (b) Hollow MSN, (c) Flu/Hollow MSN, (d) Hollow MSN-N^+CH_3, and (e) Flu/Hollow MSN-N^+CH_3. The alkylammonium-functionalized hollow mesoporous silica (Hollow MSN-N^+CH_3) exhibited characteristic peak at 1486 cm^{-1} due to the C-N bond in alkylammonium moieties in FT-IR spectrum (Figure 4d) [18,47]. The characteristic peaks due to the silica framework exhibited at 460 and 1082 cm^{-1} for Si-O-Si, 959 cm^{-1} for Si-OH [6,18,47]. Also, Hollow MSN treated at high temperature of 550 °C showed peaks due to the silica framework in a position similar to that of Hollow MSN-N^+CH_3 (Figure 4b) On the other hand, the peak caused by the C-N bond did not appear. And, as high temperature treatment causes dehydration of Si-OH groups in the silica framework, Si-OH groups are reduced by condensation to form Si-O-Si bonds [45,48]. Therefore, as shown in Figure 4b, the intensity of the FT-IR peak for Si-OH was significantly reduced. Figure 4c shows FT-IR spectrum of fludarabine-incorporated Hollow MSN (Flu/Hollow MSN) by drug solution treatment. The characteristic peaks for fludarabine in the spectrum were not observed. The result may be attributed to the low affinity between silanol groups (Si-OH) present on the surface of mesopores and fludarabine molecules containing negatively charged phosphate groups [49]. Most of the fludarabine molecules were lost during the introduction of the fludarabine molecules into the hollow MSN including the sample rinsing process. For the FT-

Preprints (www.preprints.org) | NOT PEER-REVIEWED | Posted: 24 August 2023 doi:10.20944/preprints202308.1656.v1

IR spectrum of fludarabine introduced Flu/Hollow MSN-N$^+$CH$_3$ (Figure 4e), the characteristic peak of fludarabine was not clearly observed. It is, however, the result of overlapping peak positions of fludarabine and Hollow MSN-N$^+$CH$_3$

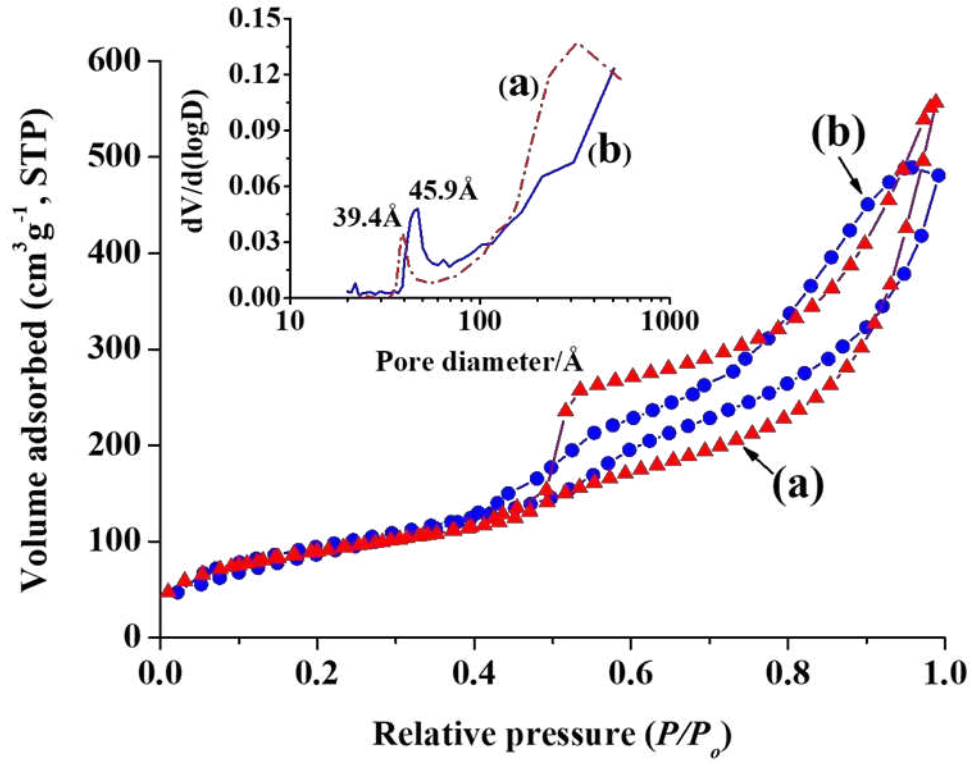

Figure 3. N$_2$ adsorption-desorption isotherms of (a) Hollow MSN and (b) Hollow MSN-N$^+$CH$_3$. Inset shows pore size distributions of (a) Hollow MSN and (b) Hollow MSN-N$^+$CH$_3$.

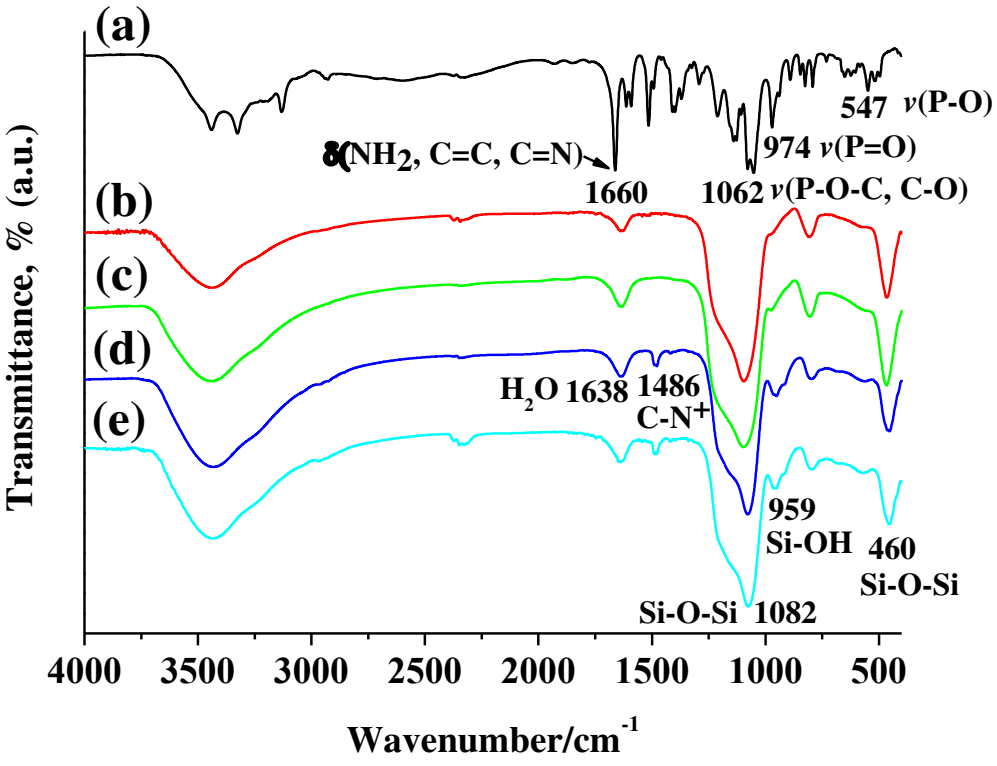

Figure 4. FT-IR spectra of (a) Fludarabine phosphate, (b) Hollow MSN, (c) Flu/Hollow MSN, (d) Hollow MSN-N$^+$CH$_3$, and (e) Flu/Hollow MSN-N$^+$CH$_3$.

Preprints (www.preprints.org) | NOT PEER-REVIEWED | Posted: 24 August 2023 doi:10.20944/preprints202308.1656.v1

3.2.5. Incorporation of fludarabine in Flu/Hollow MSN-N^+CH_3

Incorporation of fludarabine into Hollow MSN-N^+CH_3 and Hollow MSN, UV-vis technique was used to clearly identify them. The incorporated amount of fludarabine was calculated based on the UV-vis adsorption of the fludarabine solution before and after adsorption to the adsorbent. The alkylammonium-functionalized hollow mesoporous silica (Hollow MSN-N^+CH_3) had an adsorption capacity of 1.68 $molg^{-1}$ of fludarabine. On the other hand, the Hollow MSN, which does not have organic functional groups, hardly adsorbed fludarabine (Figure 5). The result agrees well with the result of the FT-IR spectrum shown in Figure 4c.

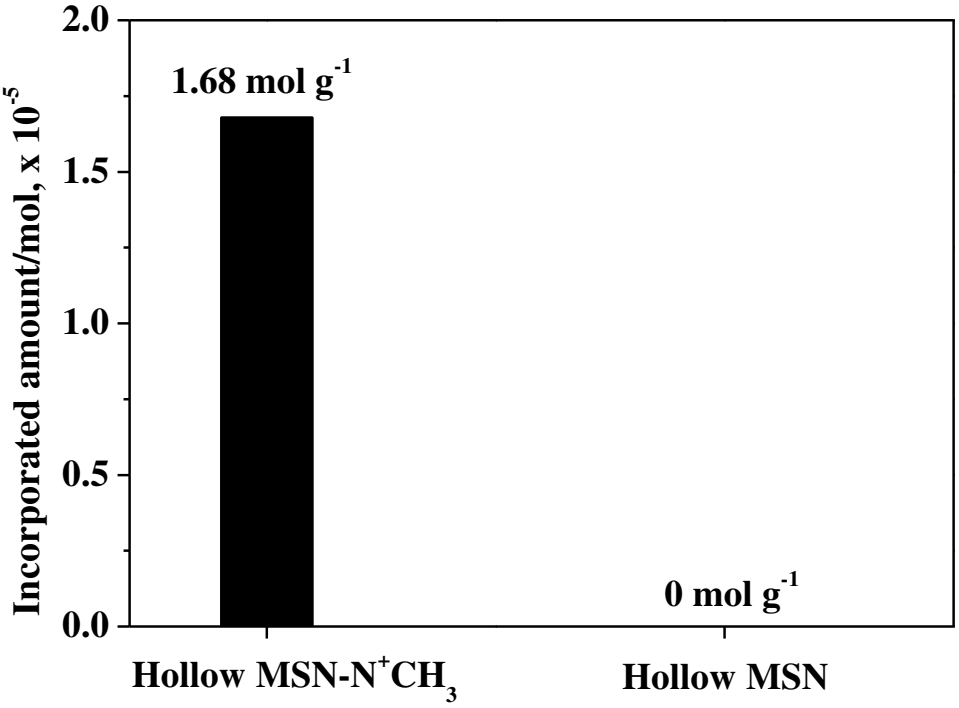

Figure 5. Incorporated amount of fludarabine in Hollow MSN and Flu/Hollow MSN-N^+CH_3.

3.2.6. Time-dependent release profiles of fludarabine

Figure 6 shows time-dependent release profiles of fludarabine from Flu/Hollow MSN-N^+CH_3, with different pH environment of (a) pH 4.8, (b) 7.4, and 9.0 at 37 °C. With the pH increase to pH 9.0, the interaction between fludarabine and the alkylammonium group would be hindered as the OH^- counter ion in solution interacts with the alkylammonium groups on the mesopore surface. Thereby the drug release amount increased at higher pH than pH 4.8.

Preprints (www.preprints.org) | NOT PEER-REVIEWED | Posted: 24 August 2023 doi:10.20944/preprints202308.1656.v1

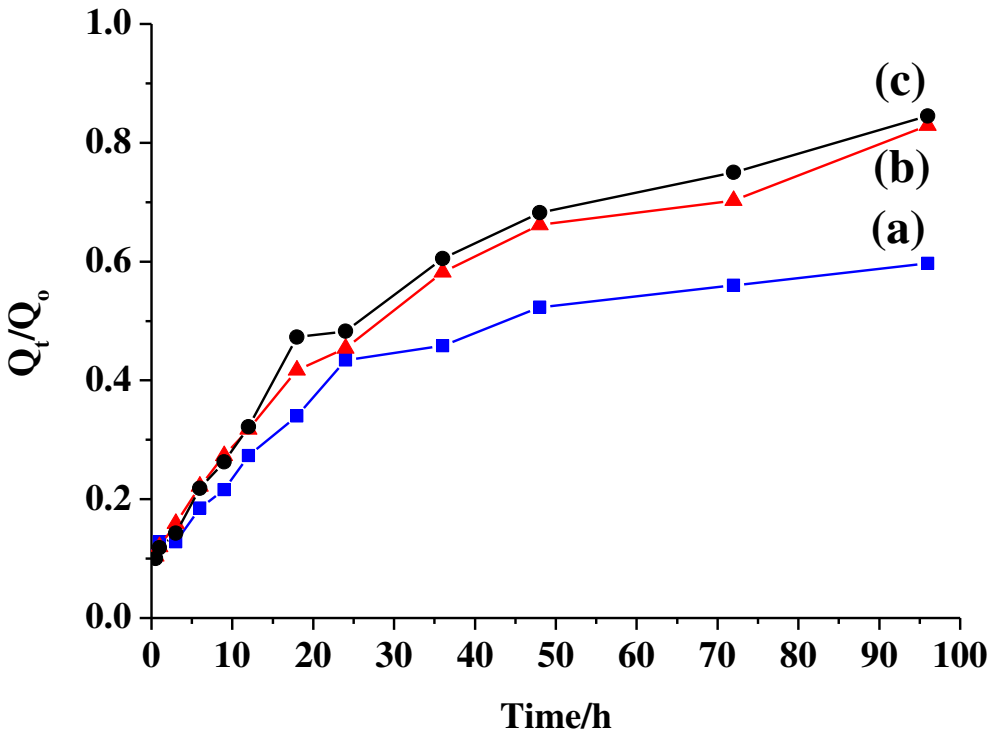

Figure 6. Time-dependent release profiles of fludarabine from Flu/Hollow MSN-N^+CH_3, with different pH environment of (a) pH 4.8, (b) 7.4, and 9.0 at 37 °C.

3.2.7. Cytotoxicity test against cancer cell

In the cancer cell viability test with MCF-7 cell, although fludarabine-incorporated mesoporous silica nanoparticles do not show much better performance than pure fludarabine, the fludarabine-incorporated hollow mesoporous silica nanoparticles show excellent cancer cell death comparable with pure fludarabine drug. One important point can be considered; When a pure drug is ingested into the body, only a small amount of the drug molecule acts on cancer cells. And the rest of the drugs will adversely affect normal cells. To solve this problem, many researchers studied controlled drug release system. In this context, the controlled fludarabine release in this work is of great significance. MCF-7 showed cell viability of 2.5% when 100 μg/ml of Flu/Hollow MSN-N^+CH_3 was dosed. The result indicates that Flu/Hollow MSN-N^+CH_3 is a proper candidate material for MCF-7 cancer cells.

Preprints (www.preprints.org) | NOT PEER-REVIEWED | Posted: 24 August 2023 doi:10.20944/preprints202308.1656.v1

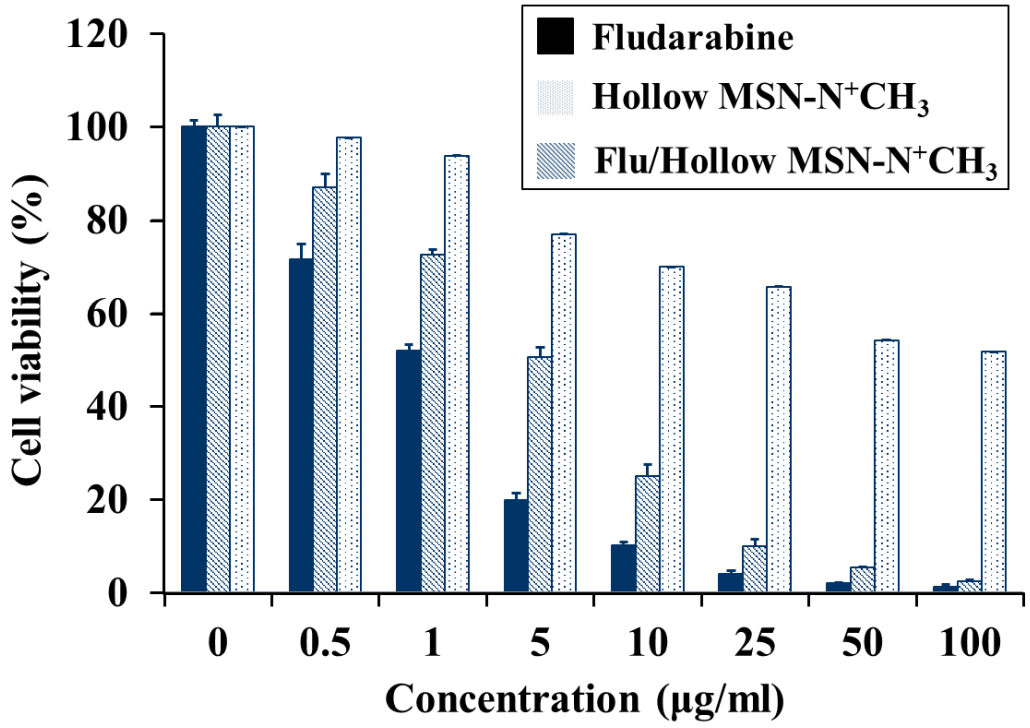

Figure 7. In vitro cytotoxicity of Flu/Hollow MSN-N^+CH_3 against MCF-7 cancer cells.

4. Conclusions

In this work, the alkylammonium-functionalized hollow mesoporous silica (Hollow MSN-N^+CH_3) nanoparticles were synthesized using zwitterionic surfactant (N-dodecyl-N,N-dimethyl-3-ammonio-1-propane sulfonate, DDAPS), anionic surfactant (sodium dodecyl sulfate, SDS), and triethanolamine as structure-directing agents, TEOS and alkylammonium alkoxysilane (TMAPS) as silica sources. The Hollow MSN-N^+CH_3 had the particle size of ca. 450 nm with the shell thickness of ca. 60 nm. The surface area and pore volume of the Hollow MSN-N^+CH_3 were 408 m^2g^{-1} and 0.8 cm^3g^{-1}, respectively, with uniform pore diameter of 45.9 Å. The Flu/Hollow MSN-N^+CH_3 containing fludarabine molecules as a model drug exhibited the controlled release behavior of drug molecules at different pH conditions (pH 4.8, 7.4, 9.0). In the cell cytotoxicity test against MCF-7 cancer cell, fludarabine-incorporated and alkylammonium-functionalized hollow mesoporous silica nanoparticles (Flu/Hollow MSN-N^+CH_3) showed the cell viability of 2.5%. The result implies the hollow The Hollow MSN-N^+CH_3 possesses a promising cancer cell killing ability comparable to pure fludarabine drug. It is considered that our current materials have the excellent applicability as pH-responsive nanocarriers in the field of medical treatment.

Author Contributions: Conceptualization, S.S.P.; methodology, S.S.P.; software, S.S.P.; validation, S.S.P. and C.-S.H.; formal analysis, S.S.P.; investigation, S.S.P. and C.-S.H.; resources, C.-S.H.; data curation, S.S.P.; writing—original draft preparation, S.S.P.; writing—review and editing, S.S.P. and C.-S.H.; visualization, S.S.P. and C.-S.H.; supervision, C.-S.H.; project administration, S.S.P. and C.-S.H.; funding acquisition, S.S.P. and C.-S.H. All authors have read and agreed to the published version of the manuscript.

Funding: The work was supported by the National Research Foundation of Korea (NRF) Grant funded by the Ministry of Science and ICT, Korea (NRF-2021R1I1A3059777, 2021R1I1A3060098).

Institutional Review Board Statement: Not applicable.

Informed Consent Statement: Not applicable.

Data Availability Statement: Not applicable.

Acknowledgments: The authors thank to Prof. Sun-Hee Kim and Mr. Moon Hyun Jung of Department of Biochemistry School of Medicine, Pusan National University Yangsan Hospital, Yangsan, 50612, Republic of Korea for their helps in performing cytotoxicity test against cancer cell.

Conflicts of Interest: The authors declare no conflict of interest.

References

1. Vargason, A.M.; Anselmo, A.C.; Mitragotri, S. The evolution of commercial drug delivery technologies. *Nat. Biomedi. Eng.* **2021**, *5*, 951-967.
2. Iwamoto, T. Clinical application of drug delivery systems in cancer chemotherapy: review of the efficacy and side effects of approved drugs. *Biol. Pharm. Bull.* **2013**, *36*, 715-718.
3. Nguyen, D.H.; Lee, J.S.; Bae, J.W.; Choi, J.H.; Lee, Y.; Son, J.Y.; Park, K.D. Targeted doxorubicin nanotherapy strongly suppressing growth of multidrug resistant tumor in mice. *Int. J. Pharm.* **2015**, *495*, 329-335.
4. Cheng, X.; Xie, Q.; Sun, Y. Advances in nanomaterial-based targeted drug delivery systems. *Front. Bioeng. Biotechnol.* **2023**, *11*, 1177151.
5. Kwon, S.; Singh, R.K.; Perez, R.A.; Neel, E.A.A.; Kim, H.-W.; Chrzanowski, W. Silica-based mesoporous nanoparticles for controlled drug delivery. *J. Tissue Eng.* **2013**, *4*, 2041731413503357.
6. Kong, J.; Park, S.S.; Ha C.-S. pH-Sensitive polyacrylic acid-gated mesoporous silica nanocarrier incorporated with calcium ions for controlled drug release. *Materials* **2022**, *15*(17), 5926.
7. Yang, P.; Gai, S.; Lin, J. Functionalized mesoporous silica materials for controlled drug delivery. *Chem. Soc. Rev.* **2012**, *41*(9), 3679-3698.
8. Slowing, I.I.; Vivero-Escoto, J.L.; Wu, C.-W.; Lin, V.S.-Y. Mesoporous silica nanoparticles as controlled release drug delivery and gene transfection carriers. *Adv. Drug Deliv. Rev.* **2008**, *60*(11), 1278-1288.
9. Theato, P.; Sumerlin, B.S.; O'Reilly, R.K.; Epps III, T.H. Stimuli responsive materials. *Chem. Soc. Rev.* **2013**, *42*(17), 7055-7056.
10. Guragain, S.; Bastakoti, B.P.; Malgras, V.; Nakashima, K.; Yamauchi, Y. Multi-stimuli-responsive polymeric materials. *Chem. Eur. J.* **2015**, *21*(38), 13164-13174.
11. Ghosn, Y.; Kamareddine, M.H.; Tawk, A.; Elia, C.; El Mahmoud, A.; Terro, K.; El Harake, N.; El-Baba, B.; Makdessi, J.; Farhat, S. Inorganic nanoparticles as drug delivery systems and their potential role in the treatment of chronic myelogenous leukaemia. *Technol. Cancer Res. Treat.* **2019**, *8*, 1-12.
12. Parra-Nieto, J.; del Cid, M.A.G.; de Carcer, I.A.; Baeza, A. Inorganic porous nanoparticles for drug delivery in antitumoral therapy. *Biotechnol. J.* **2021**, *16*, 2000150.
13. Kankala, R.K.; Han, Y.-H.; Na, J.; Lee, C.-H.; Sun, Z.; Wang, S.-B.; Kimura, T.; Ok, Y.S.; Yamauchi, Y.; Chen, A.-Z.; Wu K.C.-W. Nanoarchitectured structure and surface biofunctionality of mesoporous silica nanoparticles. *Adv. Mater.* **2020**, *32*, 1907035.
14. Li, Z.; Zhang Y.; Feng, N. Mesoporous silica nanoparticles: synthesis, classification, drug loading, pharmacokinetics, biocompatibility, and application in drug delivery. *Expert Opin. Drug Deliv.* **2019**, *16*, 219-237.
15. Murugan, B.; Sagadevan, S.; Lett J, A.; Fatimah, I.; Fatema, K.N.; Oh, W.-C.; Mohammad, F.; Johan, R.M. Role of mesoporous silica nanoparticles for the drug delivery applications. *Mater. Res. Express* **2020**, *7*, 102002.
16. Niedermayer, S.; Weiss, V.; Herrmann, A.; Schmidt, A.; Datz, S.; Müller, K.; Wagner, E.; Bein, T.; Bräuchle, C. Multifunctional polymer-capped mesoporous silica nanoparticles for pH-responsive targeted drug delivery. *Nanoscale* **2015**, *7*(17), 7953-7964.
17. Petushkov, A.; Ndiege, N.; Salem, A.K.; Larsen, S.C. Toxicity of silica nanomaterials: zeolites, mesoporous silica, and amorphous silica nanoparticles. *J. Biochem. Mol. Toxicol.* **2010**, *4*, 223-266.
18. Park, S.S.; Jung, M.H.; Lee, Y.-S.; Bae, J.-H.; Kim, S.-H.; Ha C.-S. Functionalised mesoporous silica nanoparticles with excellent cytotoxicity against various cancer cells for pH-responsive and controlled drug delivery. Mater. Des. **2019**, *184*, 108187.
19. Ma, P.; Xiao, H.; Li, C.; Dai, Y.; Cheng, Z.; Hou, Z.; Lin, J. Inorganic nanocarriers for platinum drug delivery. *Mater. Today* **2015**, *18*(10), 554-564.
20. Florek, J.; Caillard, R.; Kleitz, F. Evaluation of mesoporous silica nanoparticles for oral drug delivery–current status and perspective of MSNs drug carriers. *Nanoscale* **2017**, *9*, 15252-15277.
21. Niculescu, V.-C. Mesoporous silica nanoparticles for bio-applications. *Front. Mater.* **2020**, *7*, Article 36.
22. Murugan, B.; Sagadevan, S.; Lett, A.; Fatimah, I.; Fatema, K.N.; Oh, W.-C.; Mohammad, F.; Johan, M.R. Role of mesoporous silica nanoparticles for the drug delivery applications. *Mater. Res. Express* **2020**, *7*, 102002.
23. Gao, Y.; Gao, D.; Shen, J.; Wang, Q. A Review of Mesoporous Silica Nanoparticle Delivery Systems in Chemo-Based Combination Cancer Therapies. *Front. Mater.* **2020**, *7*, Article 598722.

24. Trzeciak, K.; Chotera-Ouda, A.; Bak-Sypien, I.I.; Potrzebowski, M.J. Mesoporous silica particles as drug delivery systems—The state of the art in loading methods and the recent progress in analytical techniques for monitoring these processes. *Pharmaceutics* **2021**, *13*, 950.
25. Vallet-Regí, M.; Schüth, F.; Lozano, D.; Colilla, M.; Manzano, M. Engineering mesoporous silica nanoparticles for drug delivery: where are we after two decades?. *Chem. Soc. Rev.*, **2022**, *51*, 5365-5451.
26. Ma, X.; Zhao, Y.; Ng, K.W.; Zhao Y. Integrated hollow mesoporous silica nanoparticles for target Drug/siRNA co-delivery. *Chem. Eur. J.* **2013**, *19*(46), 15593-15603.
27. Liu Y.; Chen Q.; Xu, M. Guan, G., Hu, W. Liang Y, Zhao X, Qiao M, Chen D, Liu H Single peptide ligand-functionalized uniform hollow mesoporous silica nanoparticles achieving dual-targeting drug delivery to tumor cells and angiogenic blood vessel cells. *Int. J. Nanomedicine* **2015**, 101855-67.
28. Chakravarty, R.; Goel, S.; Hong, H.; Chen, F.; Valdovinos, H.; Hernandez, R.; Barnhart, T.E.; Cai W. Hollow mesoporous silica nanoparticles for tumor vasculature targeting and PET image-guided drug delivery. *Nanomedicine* (Lond), **2015**, *10*(8), 1233-1246.
29. She, X.; Chen, L.; Li, C.; He, C.; He, L.; Kong L. Functionalization of hollow mesoporous silica nanoparticles for improved 5-FU loading. *J. Nanomater* **2015**, *2015*, Article ID 872035.
30. Yang, J.; Lee, J.; Kang, J.; Lee, K.; Suh, J.-S.; Yoon, H.-G.; Huh, Y -M.; Haam S. Hollow Silica Nanocontainers as Drug Delivery Vehicles. *Langmuir* **2008**, *24*, 7, 3417-3421.
31. Xu, T.; Shan, C.; Ran, M.; Shuai, Z.; Longyan, Y.; Qian, M.; Wenguo, J.; Junqi, H. Hollow silica nanocontainers as drug delivery vehicles. *J. Nanosci. Nanotechnol.* **2015**, *15*(5), 3773-3779.
32. Zhu, Y.; Fan, Y.; Borchardt, L.; Kaskel S. PEGylated hollow mesoporous silica nanoparticles as potential drug delivery vehicles. *Micropor. Mesopor. Mater.* **2011**, *141*(1-3), 199-206.
33. Liu, J.; Li, Y.; Zhao, M.; Lei, Z.; Guo, H.; Tang, Y.; Yan H. J. Biomater. Sci. **2020**, *31*, 472-490.
34. Nia, M.H.; Koshani, R.; Munguia-Lopez, J.G.; Kiasat, A.R.; Kinsella, J.M.; van de Ven, T.G.M. Biotemplated hollow mesoporous silica particles as efficient carriers for drug delivery. *ACS Appl. Bio Mater.* **2021**, *4*(5), 4201-4214.
35. Li, Q.; Liu, Q.; Li, H.; Dong, L.; Zhou, Y.; Zhu, J.; Yang, L.; Tao, J. Modified hollow mesoporous silica nanoparticles as immune adjuvant-nanocarriers for photodynamically enhanced cancer immunotherapy. *Front. Bioeng. Biotechnol*. **2022**, *10*, 1039154.
36. Porrang, S.; Davaran, S.; Rahemi, N.; Allahyari, S.; Mostafavi, E. How advancing are mesoporous silica nanoparticles? A comprehensive review of the literature. Int. J. Nanomedicine **2022**, *17*, 1803-1827.
37. Watermann, A.; Brieger, J. Mesoporous silica nanoparticles as drug delivery vehicles in cancer. *Nanomaterials* **2017**, *7*, 189.
38. Isa, E.D.M.; Ahmad, H. Rahman, M.B.A.; Gill, M.R. Progress in mesoporous silica nanoparticles as drug delivery agents for cancer treatment. *Pharmaceutics* **2021**, *13*, 152.
39. Corma, A.; Botella, P.; Rivero-Buceta, E. Silica-based stimuli-responsive systems for antitumor drug delivery and controlled release. *Pharmaceutics* **2022**, *14*, 110.
40. Zhang, C.; Xie, H.; Zhang, Z.; Wen, B.; Cao, H.; Bai, Y.; Che, Q.; Guo, J.; Su, Z. Applications and biocompatibility of mesoporous silica nanocarriers in the mesoporous silica nanocarriers in the field of medicine. *Front. Pharmacol.* **2022**, *13*, Article 829796.
41. Moodley, T.; Singh, M. Polymeric mesoporous silica nanoparticles for enhanced delivery of 5-fluorouracil in vitro. *Pharmaceutics* **2019**, *11*(6), 288.
42. Saroj, S.; Rajput, S.J.; Tailor-made pH-sensitive polyacrylic acid functionalized mesoporous silica nanoparticles for efficient and controlled delivery of anti-cancer drug etoposide. *Drug Dev. Ind. Pharm.* **2018**, *44*(7), 1198-1211.
43. Park, S.S.; Moorthy, M.S.; Song, H.-J.; Ha, C.-S. Functionalized mesoporous silicas with crown ether moieties for selective adsorption of lithium ions in artificial sea water. *J. Nanosci. Nanotechnol.* **2014**, *14*, 8845-8851.
44. Park, S.S.; An, B.; Ha, C.-S. High-quality, oriented and mesostructured organosilica monolithas a potential UV sensor. *Microporous Mesoporous Mater.* **2008**, *111*, 367-378.
45. Park, S.S.; Jung, Y.; Xue, C.; Che, R.; Zhao, D.; Ha, C.-S. Free-standing mesoporous silica/carbon composite films with crystalline silica wallfrom ethylene-bridged organosilane. *Chem. Mater.* **2010**, *22*, 18-26.
46. Park, S.S.; Ameduri, B.; Ha, C.-S. One-pot synthesis of alkylammonium-functionalized mesoporous silica hollow spheres in water and films at the air–water interface. *Emergent Materials* **2019**, 2, 45-58.
47. Park, S.S.; Kong, J.; Selvaraj, M.; Ha, C.-S. Functionalized mesoporous silica for highly selective sensing of iron ion in water. J. Nanosci. Nanotechnol. **2001**, *21*, 4406-4411.
48. Suteewong, T.; Sai, H.; Cohen, R.; Wang, S.; Bradbury, M.; Baird, B.; Gruner, S.M.; Wiesner, U. Highly aminated mesoporous silica nanoparticles with cubic pore structure. *J. Am. Chem. Soc.* **2011**, *133*, 172-175.
49. Elliott, T.S.; Slowey, A.; Ye, Y.; Conway, S.J. The use of phosphate bioisosteres in medicinal chemistry and chemical biology. *Med. Chem. Commun.* **2012**, *3*, 735-751.